Solvent mobility in poly(methyl methacrylate)/toluene solutions by depolarized and polarized light scattering

G. Floudas, G. Fytas, and W. Brown

Citation: The Journal of Chemical Physics **96**, 2164 (1992); doi: 10.1063/1.462068
View online: http://dx.doi.org/10.1063/1.462068
View Table of Contents: http://scitation.aip.org/content/aip/journal/jcp/96/3?ver=pdfcov
Published by the AIP Publishing

Solvent mobility in poly(methyl methacrylate)/toluene solutions by depolarized and polarized light scattering

G. Floudas[a),b)] and G. Fytas
Research Center of Crete, P.O. Box 1527, 711 10 Heraklion Crete, Greece

W. Brown
Institute of Physical Chemistry, University of Uppsala, P.O. Box 532, 75121 Uppsala, Sweden

(Received 25 June 1991; accepted 15 October 1991)

Depolarized Rayleigh and polarized Rayleigh–Brillouin scattering are employed to examine the mobility of toluene in solutions of poly(methyl methacrylate) (PMMA) and for PMMA concentrations: $0 \leqslant c_{PMMA} \leqslant 1$. The depolarized Rayleigh measurements were performed in the temperature range 20–120 °C with several interferometer spacings, whereas the polarized Rayleigh–Brillouin measurements were made in the range from − 20 to 140 °C. The reorientation times of toluene, obtained from a single Lorentzian fit to the experimental depolarized spectra, are in good agreement with earlier NMR and dielectric relaxation data. Two Lorentzians were necessary to fit the depolarized spectra of the PMMA/toluene solutions at all temperatures. The broader Lorentzian is due to fast toluene reorientation and the narrower Lorentzian contains contributions from both slowly relaxing polymer chains and slow solvent reorientation in the macromolecular environment. The reorientation time and the fraction of the "mobile" toluene molecules are obtained, respectively, from the width and the integrated intensity of the broader Lorentzian. We discuss the reorientational dynamics of the broader Lorentzian with respect to the normalized solvent relaxation time τ/τ_0, where τ_0 refers to the neat solvent. The principal conclusions of this work with respect to solvent dynamics are (i) the exponential concentration dependence of τ/τ_0 at high temperatures and for polymer concentration up to 70% which is similar for the three polymer/solvent systems employed so far, (ii) the presence of two time scales for the solvent reorientation in these homogeneous polymer solutions, and (iii) these "fast" and "slow" relaxation processes resemble the toluene and PMMA bare dynamics, respectively, and their relative amplitudes depend on temperature. The experimental results are discussed in terms of recent models of orientational relaxation in dense systems. Furthermore, the polarized Rayleigh–Brillouin measurements on the PMMA/toluene system revealed the presence of significant rotational mobility of toluene acting as an initiator for the broad hypersonic attenuation observed at GHz frequencies.

I. INTRODUCTION

The study of rotational relaxation of solute molecules in dense polymer systems has recently been intensified. Solvent molecules can undergo restricted reorientation in high-molecular-weight polymer matrices, as inferred from dielectric relaxation (DR),[1,2] H^2 and recent two-dimensional solid state NMR,[3,4] depolarized Rayleigh scattering (DRS),[5,6] and Brillouin scattering (BS).[7] Additionally, viscoelastic,[8,9] oscillatory electric birefringence (OEB),[10] NMR,[3] and DRS,[11] experiments provide evidence that the solvent properties are modified by the presence of polymer chains. To explain the alteration of solvent properties, theoretical models of rotational relaxation[12,13] and molecular dynamics simulations[14] were subsequently employed.

Viscoelastic[8,9] and oscillatory shear birefringence experiments,[10] in a variety of polymer/solvent systems, demonstrated that subtraction of the solvent contribution from the high-frequency limiting solution viscosity η'_∞ and birefringence S'_∞ resulted in a quantity—which has traditionally been interpreted as due mainly to the polymer—which does not approach zero at high frequencies. Consequently, it has been suggested that the observed high-frequency behavior may predominantly reflect the modification of the solvent properties by the polymer. Recently, the rotational relaxation of the solvent Aroclor (A1248) in solutions containing polystyrene (PS) with PS concentration c_{PS} $0 \leqslant c_{PS} \leqslant 0.27$ g/cc and 1,4 polybutadiene (PB) with PB concentration $0 \leqslant c_{PB} \leqslant 0.26$ g/cc has been examined by OEB.[10] In both cases, the normalized solvent relaxation time τ/τ_0, where τ_0 refers to the neat solvent relaxation time, was found to exhibit an exponential dependence on concentration. This ratio can be used as a measure of an average local friction that the solvent molecules experience in the vicinity of the polymer chains. It is thus of primary importance to obtain this ratio at higher polymer concentrations. The reorientational dynamics of the same solvent (A1248) have also been studied by DRS.[11] For PS/A1248 solutions, the analysis of the experimental depolarized spectra was based on the assumption of two distinct Lorentzian peaks. The variation of the integrated intensities with temperature and PS concen-

[a)] Present address: Imperial College, Department of Chemical Engineering, London SW7 2BY.
[b)] Author to whom correspondence should be addressed.

 0021-9606/92/032164-11$06.00

tration suggest the presence of two solvent populations: one "mobile" and one "hindered" by the PS chains. Albeit, a distribution of Lorentzians is conceivable for modified solvent reorientation—also implied by recent photon correlation spectroscopy (PCS) measurements[15] at low temperatures—its extraction from the experimental depolarized spectra is not possible. Even a good double Lorentzian fit may yield ambiguous results beyond certain limits for the contribution of the narrow and broad Lorentzian to the depolarized spectra. It is therefore crucial to support the findings of the PS/A1248 investigation, employing another system and concurrently improving the experimental conditions.

The purpose of the present study is to investigate solvent relaxation (toluene) within a high molecular weight polymer matrix (PMMA) over a range of temperature and polymer concentration. The effect of polymer on the microscopic dynamics of the solvent can best be examined by selective probing of the solvent. Thus, we employ depolarized Rayleigh scattering for bulk PMMA, neat toluene, and PMMA/toluene mixtures in the temperature range 20–120 °C. We complement our results with polarized Rayleigh–Brillouin measurements made on the same system in the temperature range from −20 to 140 °C.

The PMMA/toluene system was chosen for the present study for two reasons: Firstly, because PMMA and toluene are nearly refractive index matched; secondly because toluene has a much higher depolarized intensity than that of PMMA. The first observation minimizes the contribution from unwanted concentration fluctuations to the scattered intensity, whereas the second preserves the selectivity of DRS. Due to the very fast reorientation time (few ps) of toluene, the solute (PMMA) contribution can be separately measured at a small free spectral range (FSR). Moreover, PMMA and toluene are miscible in all proportions and a study can be made at high polymer concentrations.

II. EXPERIMENTAL SECTION

The depolarized Rayleigh spectra $I_{VH}(\omega)$ were obtained at a scattering angle of 90° using the apparatus described elsewhere.[11] Four free spectral ranges (FSR) were used; 228, 146, 40, and 9.7 GHz, with a finesse in excess of 65 for all depolarized spectra. The data analysis consisted of fitting each peak to either a single Lorentzian (neat solvent) or a double Lorentzian (PMMA/toluene solutions) plus a baseline:

$$I_{VH}(\omega) = \frac{1}{\pi} \sum_{i=1}^{2} I_i \frac{\Gamma_i}{\Gamma_i^2 + \omega^2} + B, \qquad (1)$$

where I_1 and I_2 are the integrated intensities of the narrower and broader interferometric components, respectively, Γ_1 and Γ_2 are the corresponding half-widths at half-height (HWHH), and B is the background. All depolarized spectra were then convoluted with the instrument line shape and the HWHH and the integrated intensity of each Lorentzian was then calculated by the fitting program. The collective reorientation time was then computed from $\tau_2 = (2\pi\Gamma_2)^{-1}$. An alternative fitting procedure to the experimental spectra would be to fit each spectrum with a continuous distribution of Lorenztians implied by the notion of a modified solvent reorientation in accord with the PCS results on the systems PS/A1248 and PB/A1248.[15] This procedure was not employed here for two reasons: Firstly, because the reorientation time τ_2 was highly reproducible at a given temperature with the aforementioned procedure and, hence, yielded physically meaningful temperature dependence; secondly, because it was insensitive to the FSR employed at all temperatures.

DRS spectra were recorded in the temperature range from 20 to 120 °C. Typical $I_{VH}(\omega)$ spectra for bulk PMMA, neat toluene, and a PMMA/toluene solution with $c_{PMMA} = 0.3$ g/cc are shown in Fig. 1. Two intriguing features emerge from Fig. 1. First, the reorientational dynamics of neat toluene (in the ps time scale) are much faster than the PMMA times (in the ns or longer time scale) and these time scales persist in the PMMA/toluene mixtures [Fig. 1(c)]. Second, we notice the large difference in the integrated intensities which is proportional to the effective optical anisotropy[16,17] $\gamma_{\rm eff}^2$:

$$I_{VH} = A f(n) \rho^* \gamma_{\rm eff}^2, \qquad (2)$$

where A is a constant, $f(n)$ is the product of the local field correction and the geometrical factor $1/n^2$, with n being the refractive index, and ρ^* the number density of solute. Using the reported Rayleigh ratio for toluene[17] and $\rho = 0.867$ g/cc and $n = 1.496$ for the density and refractive index, respectively, we obtain an effective optical anisotropy of 23 Å^6 for toluene. This value should be compared with the average optical anisotropy per PMMA monomer of $\langle \gamma^2 \rangle / x = 1$ Å^6 (where x is the degree of polymerization). Evidently, a monomer in an isolated PMMA chain is more than 20 times less

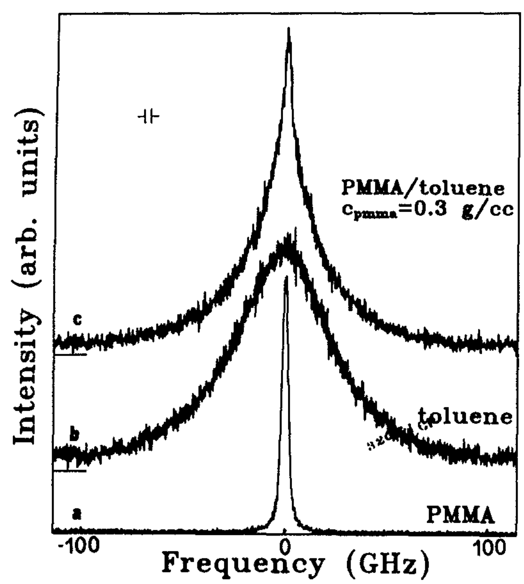

FIG. 1. Depolarized Rayleigh spectra of PMMA, toluene, and PMMA/toluene with a PMMA concentration of 0.3 g/cc at 20 °C, obtained in consecutive runs. The symbol in the upper left-hand corner denotes the instrument full width.

effective an anisotropic scatterer as a toluene molecule in the neat solvent.

Polarized Rayleigh–Brillouin spectra $[I_{VV}(\omega)]$ were recorded in the temperature range from -20 to 140 °C at a scattering angle of 90° using a single-pass piezoelectrically scanned plane Fabry–Perot interferometer (Tropel 350) with a FSR of 27.3 GHz and a finesse of about 50. After repeated collection, two spectral orders were transferred to a VAX computer for further analysis. The $I_{VV}(\omega)$ spectra consist of two central components and two shifted Brillouin peaks. The unshifted line corresponds to the resolution function and the "mountain" peak. The *VH* contribution to the polarized spectra appears as a flat background due to the much faster reorientational motion of the solvent. Indeed, we witnessed an increasing background in the $I_{VV}(\omega)$ spectra with increasing toluene concentration.

Figure 2 shows $I_{VV}(\omega)$ for neat toluene, bulk PMMA, and a PMMA/toluene mixture with $c_{\mathrm{PMMA}} = 0.7$ g/cc at 60 °C. The two Brillouin peaks are shifted from the incident frequency by an amount $\omega_B = qu(q)$, where q is the wave vector and $u(q)$ the sound velocity. Sound waves are attenuated in the sample resulting in a linewidth (HWHH): $\Gamma_B = \alpha u(q)/2\pi$, where α is the attenuation coefficient. Usually, the hypersonic loss is expressed as $\tan\delta = 2\Gamma_B/f_B$. In the present study, the Brillouin peaks were represented by a Lorentzian shape and a nonlinear least-squares fitting program was employed to calculate Γ_B and f_B. The true Γ_B, was obtained after subtraction of the instrument line width.

The Landau–Placzek (LP) intensity ratio, i.e., the ratio of the unshifted spectral component to the intensity of the Brillouin doublets is often used as a measure of optical quality of amorphous polymeric materials. For the bulk and plasticized PMMA used in the present study, the LP ratio was less than 4 at all temperatures. This is, to our knowledge, one of the lowest LP ratio's reported for bulk PMMA.[18] Recently, a study[19] of highly syndiotactic poly(n-butyl methacrylate) (PBMA) revealed low LP ratio's as a result of the homogeneous stereochemistry of the sample.

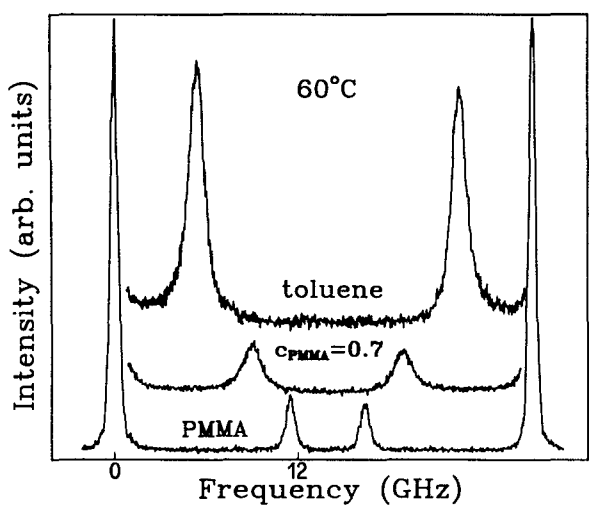

FIG. 2. Polarized Rayleigh–Brillouin spectra of PMMA, a PMMA/toluene mixture with PMMA concentration of 0.7 g/cc, and neat toluene, at 60 °C, obtained in consecutive runs.

The PMMA and PMMA/toluene samples were prepared by thermal polymerization, giving an atactic product. Care was taken to prevent internal stresses in the polymer. The samples consist of toluene and high MW PMMA ($\sim 1\times 10^5$ and 4×10^5 for the low and high c_{PMMA} samples,[20] respectively, with polydispersity of ~ 2) with concentrations of 1, 0.9, 0.8, 0.7, 0.6, 0.5, 0.4, 0.3, 0.2, and 0.1 g/cc in PMMA. The glass transition temperature of bulk PMMA was 380 K and the corresponding T_g's of the plasticized PMMA with $c_{\mathrm{PMMA}} = 0.9$ and 0.8 g/cc were, respectively, 356 and 353 K as measured by DSC (heating rate 20 °C/min). It is worth mentioning that although, for $c_{\mathrm{PMMA}} = 0.9$ g/cc, the transition range was similar to bulk PMMA ($\Delta T_g \sim 20$ K), for the sample with $c_{\mathrm{PMMA}} = 0.8$ g/cc we witnessed a broader transition range due to plasticization.[21] Glass transition temperatures are also reported in Ref. 22.

III. RESULTS AND DISCUSSION

A. Depolarized Rayleigh scattering

1. Neat solvent reorientation

The neat solvent $I_{VH}(\omega)$ spectra [Fig. 1(b)] are well described by a Lorentzian peak plus a baseline. The central "dip," characteristic of some glass formers,[23] will only appear at much lower temperatures (-80 °C) than the temperatures employed in the present study.[24] The reorientation time depends on the macroscopic viscosity via the modified Stokes–Einstein–Debye (SED) equation:[25]

$$\tau_0 = \frac{g_2}{j_2}\left(\frac{V_h}{k_B}\frac{\eta_s}{T}\right) + \tau_\infty , \tag{3}$$

where V_h is the effective hydrodynamic volume of the reorienting molecule, η_s is the shear viscosity, g_2 is the static pair orientation correlation function, j_2 is the dynamic pair orientation correlation function (usually assumed to be 1), and τ_∞ is the nonzero intercept necessary to fit the relaxation times. The physical meaning of the intercept, if any, is as yet not clear. To interpret the presence of a nonzero intercept in the SED equation, hypotheses have been made about the nonlinearity of the τ_0 versus η_s/T plots. A recent study of simple supercooled liquids[26] demonstrated strong deviations from the SED equation below a critical temperature T_c ($T_c \approx 1.18 T_g$). At higher temperatures—in the fluid regime—the SED equation was found to be valid, but at lower temperatures—in the viscous regime—it was found that the viscosity increases more strongly than the reorientation time, implying a breakdown of the SED equation. This was demonstrated[27] by a discontinuity in the plot of τ/η_s versus T_g/T for a number of supercooled liquids and was attributed to a change in the diffusion mechanism at the critical temperature T_c. Moreover, in a recent study[11] of the solvent Aroclor (A1248), a breakdown of the SED equation was demonstrated and attributed to a considerable amount of orientational pair correlations. These experimental evidences favor the concept of a dynamic phase transition at the

temperature T_c, as predicted by recent mode coupling theory.[28] On the other hand, from a similar plot for toluene (τ_0/η_s versus T_g/T, not shown here), no definite conclusions could be made mainly because of lack of viscosity measurements at temperatures close to T_g (see Fig. 3).

In the absence of strong solute-solvent interactions, slip boundary conditions can successfully predict the reorientation time of most small molecules.[29] Under such conditions the hydrodynamic volume V_h is less than the volume V_z swept out by the reorientation of the symmetry axis z by a factor which is calculated from the axial ratio ρ: the ratio of the shorter to the z axis for prolate and oblate ellipsoids. From the experimental reorientation times with the use of the modified SED equation [Eq. (3)], we can extract an estimate for the effective hydrodynamic volume of toluene. In doing so, the temperature dependence of the shear viscosity is needed in Eq. (3). The reported[30] temperature dependence of the shear viscosity is described by the Vogel–Fulcher–Tamman (VFT) equation,

$$\log \eta = \log \eta^* + \frac{B_\eta}{T - T_0}, \tag{4}$$

with parameters $\eta^* = 6.98\times10^{-4}$P, $B_\eta = 178$ K, and $T_0 = 103.1$ K. Using Eq. (4) and the experimental reorientation times, we obtain from Eq. (3),

$$\tau_0 = 1.358\times10^{-12}\ \text{s} + \frac{\eta}{T}\,2.09\times10^{-9}\,\frac{\text{sK}}{\text{cP}}. \tag{5}$$

From the slope of Eq. (5), we deduce an effective hydrodynamic volume [$g_2 V_h$ in Eq. (3)] of ~ 30 Å^3, in good agreement with the value reported earlier.[31] This value can be reproduced using the molecular volume and the axial ratio of toluene.

Figure 3 shows the reorientation times for neat toluene in an Arrhenius plot obtained by DRS, NMR,[32] and DR.[22] The viscosity dependence is also shown for comparison. It is noteworthy that different techniques probe the same molecular motion in different time scales. Moreover, the ratio $\tau(l=1)/\tau(l=2)$ [where $\tau(l)$ is the reorientation time for the lth order spherical harmonic) is 1 and not 1/3, in agreement with earlier experimental data for toluene[31] and recent models of rotational relaxation.[33] On the contrary, previously reported depolarized Rayleigh reorientation times for toluene[24] deviate from those shown in Fig. 3, probably due to the lower reliability of the experimental times at low temperatures. The τ_0 values for neat toluene shown in Fig. 3 conform to the Vogel–Fulcher–Tamman–Hesse (VFTH) expression:

$$\log \tau_0 = \log \tau_\delta^* + \frac{B}{T - T_0} \tag{6}$$

which is equivalent to Eq. (5). A least-squares fit of Eq. (6) to the data in Fig. 3 yields $\tau_\delta^* = 0.28 \pm 0.06$ ps, $T_0 = 96 \pm 2$ K, and $B = 251 \pm 20$ K. B is about 30% higher than B_η ($= 178$ K), but this is probably due to the much narrower temperature range of the viscosity data compared to the NMR and DRS data.

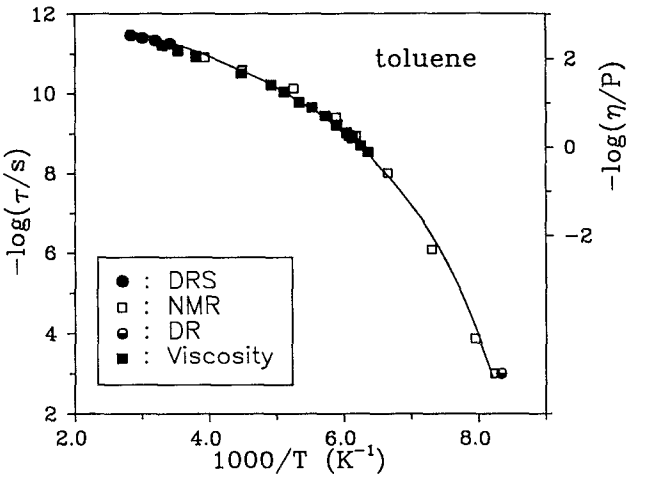

FIG. 3. Temperature dependence of the reorientational relaxation times of toluene obtained by depolarized Rayleigh scattering (●), NMR (□), and dielectric relaxation (◒). Viscosities (■) are also shown for comparison.

2. Solvent reorientation in the presence of PMMA

The temperature dependence of the reorientation time τ_0 for neat toluene and the faster reorientation time τ_2 for PMMA/toluene mixtures is depicted in Fig. 4. For low PMMA concentrations, although the macroscopic shear viscosity increases by orders of magnitude, there is only a small "slowing-down" effect on the fast reorientational relaxation. For the higher polymer concentrations there is a noticeable "slowing-down" effect which persists to the highest mea-

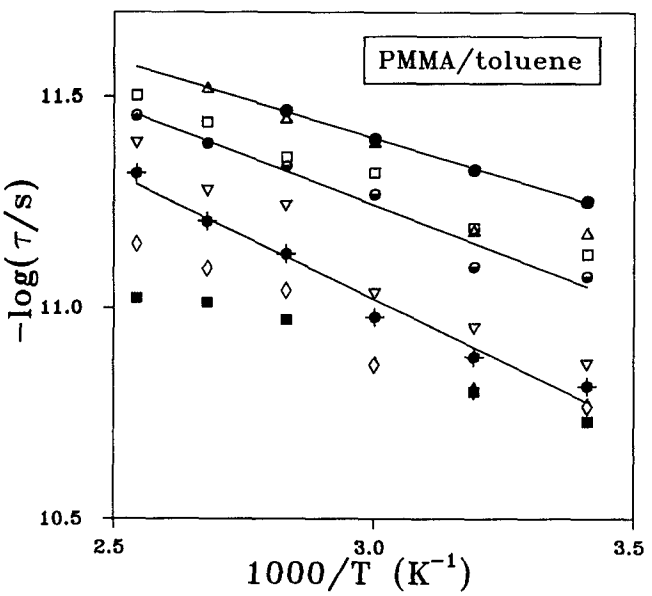

FIG. 4. Temperature dependence of the reorientational relaxation times of toluene in the undiluted state (●) and in PMMA/toluene solutions with different PMMA concentrations: △, 0.1; □, 0.2; ◒, 0.3; ▽, 0.4; ✦, 0.5; ◇, 0.6; ■, 0.7 g/cc.

surement temperatures. For $c_{PMMA} = 0.7$ g/cc, the solvent reorientation time is about 4 times longer than in the neat toluene. On the contrary, for the PMMA/chlorobenzene (CB) system,[6] no measurable influence of PMMA on the reorientation of CB was reported at high temperatures. Similarly, for the PS/styrene system,[34] the orientational rate of styrene was reduced by about 50% in the presence of 80% PS.

We now examine the concentration dependence of the fast reorientation time $\tau(c,T)$ with respect to the neat solvent time τ_0. In Fig. 5, the values of τ/τ_0 are plotted semilogarithmically versus polymer concentration for the PMMA/toluene solutions. The ratio τ/τ_0 increases markedly with increasing PMMA concentration. In fact, τ/τ_0, which defines an average local friction that the solvent molecules experience in the vicinity of the polymer chains, exhibits, at high temperatures, an exponential dependence on concentration, in agreement with viscoelastic measurements on several polymer solutions. Although this observation was made recently from OEB (Ref. 10) measurements on the systems PS/A1248 and 1,4PB/A1248, it is the first time, to our knowledge, that this prediction for τ/τ_0 is verified for polymer concentrations as high as 0.7 g/cc. In this context it is worth mentioning that a similar concentration dependence of the effective friction coefficient was recently observed in the PS/di-2-ethylhexyl phthalate (DOP) system[35] with c_{PS} up to 0.5 g/cc. In contrast to free volume considerations [Eq. (6)], the rate of increase of τ/τ_0 with PMMA concentration is rather insensitive to temperature variations over the range 20–80 °C (Fig. 5). The rate of change of solvent friction with polymer concentration is depicted in Fig. 6. Notwithstanding the different chemical nature of the solvent used, the three systems display very close

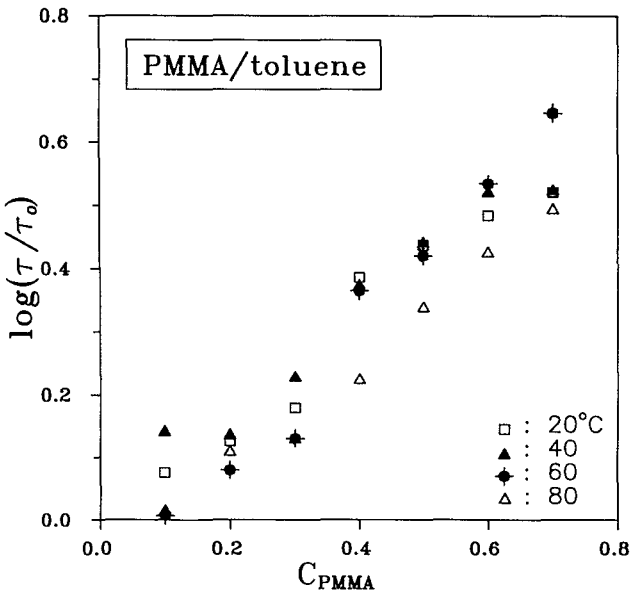

FIG. 5. Reduced solvent relaxation times vs PMMA concentration at four temperatures as indicated.

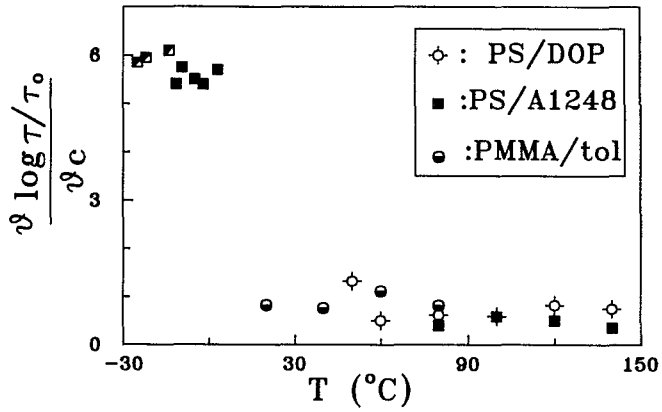

FIG. 6. The rate of change of solvent friction (τ/τ_0) with polymer concentration against temperature for PMMA/toluene (◒), PS/DOP (◈), and PS/A1248 (■) systems investigated by Fabry–Perot interferometry (FPI) at high temperatures. For the PS/A1248 system, the previously reported low-temperature PCS (◩) and OEB (■) results are also included.

$\partial \log(\tau/\tau_0)/\partial c$ values. Moreover, the three solvents in Fig. 6 possess greatly different T_g's.

Recently, the ratio R_a of the rotational friction coefficient of the solvent to its value in the neat solvent was calculated[12] as

$$R_a = 1 + bV_h[\eta]c, \tag{7}$$

where $b = 1/(b^*)^3$ (b^* is the closest distance between solvent-polymer bead). According to Eq. (7), $R_a(c)$ increases with polymer concentration at a rate depending on the product of the polymer intrinsic viscosity and the hydrodynamic volume of the solvent. For small polymer concentrations Eq. (7) can be approximated by an exponential dependence on c; for the higher polymer concentrations employed here Eq. (7) is not valid. Moreover, with respect to Fig. 6, the rate of change of solvent friction with polymer concentration at high temperatures does not depend on the hydrodynamic volume of the solvent. This is clearly demonstrated in Fig. 6 where two polymers and three solvents are employed. PS and PMMA have different structures but similar T_g's, whereas DOP, A1248, and toluene have different hydrodynamic volumes and different T_g's. The rate of change of solvent friction with polymer concentration at high temperatures studied by Fabry–Perot interferometry (FPI) is independent of the nature of the solvent, for the three solvents employed.

Apart from the reorientational dynamics, there is much valuable information in the intensities of the narrow (I_1) and broad (I_2) Lorentzians [Eq. (1)]. The intensity ratio $K = I_2/I_1$ is depicted in Fig. 7 as a function of temperature for different PMMA concentrations. If we assume, at least for the highest temperatures, that the narrow and broad spectral components arise entirely from slow segmental relaxation of PMMA and fast solvent reorientation, respectively, the computed [using Eq. (2)] K_c values exceed considerably the corresponding K's of Fig. 7. For example, for $c_{PMMA} = 0.1$ g/cc at 120 °C, $K_c \sim 210$, whereas from the fitted I_1 and I_2 [Eq. (1)] values, $K = 45$; for $c_{PMMA} = 0.2$

g/cc again at 120 °C, $K_c \sim 90$, compared with the fitted $K = 25$. At low PMMA content ($c_{PMMA} \leqslant 0.3$ g/cc) and, hence, large K_c (>50) the fit of Eq. (1) to simulated double Lorentzian spectra have shown that K is underestimated mainly through an increase of I_1, the intensity of the narrow component.[36] This can partially account for the observed difference between K_c and K only at low c_{PMMA}. For the lower K_c (<50), the fit of Eq. (1) is unique, whereas the fitted K values of Fig. 7 are smaller than K_c at all temperatures and c_{PMMA} presently considered. To elaborate this point, we took extra precautions in measuring the integrated intensities I_1 and I_2 relative to toluene. We recall here that in the PS/A1248 system ($c_{PS} \leqslant 0.15$ g/cc), an interesting interplay between I_1 and I_2 was observed.[11] To check the fitting results, it would be desirable to obtain I_1 independently. The intensity I_1 can also be obtained at small FSR's for which the broad component appears as an unresolved background. Figure 8 shows the variation of the normalized intensity $I_2^* = I_2/(I_1 + I_2)$ as a function of PMMA concentration at three temperatures. The dashed-dotted line in Fig. 8 denotes the expected variation of I_2^* without modification (dilution effect). As indicated, the extra decrease in the intensity ratio K is produced, in part, by the decrease in the intensity I_2 of the broader component. Furthermore, the decrease in I_2 is temperature dependent (Fig. 8) and it is this dependence of I_2 on temperature which creates the features observed in Fig. 7. To justify this explanation we plot in Fig. 8 the intensity of the narrower component I_1 at 60 °C. If the intensity I_1 was solely due to slowly moving polymer segments then it should be very low and additionally display a linear dependence on PMMA concentration. Instead, Fig. 8 shows that I_1 depends on polymer concentration in a strongly nonlinear manner. We recall that the intensity I_1 shown in Fig. 8 was obtained with the smallest FSR (9.7 GHz) so that the broader interferometric component appeared as a flat background.

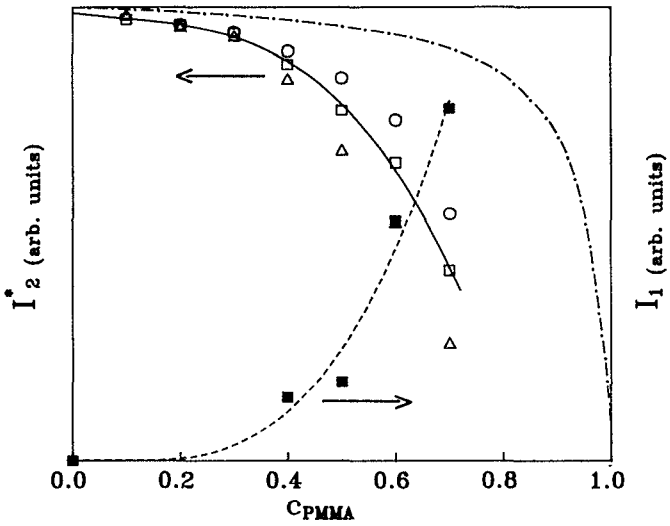

FIG. 8. Concentration dependence of the intensity $I_2^* = I_2/(I_1 + I_2)$ of the broader interferometric component at three temperatures (○, 120 °C; □, 60 °C; △, 20 °C), measured with a free spectral range of 228 GHz. The dashed-dotted line denotes the expected variation of I_2^* without modification (see text). The corresponding dependence of the intensity I_1 of the narrower interferometric component at 60 °C (■), measured with a free spectral range of 9.7 GHz, is also shown.

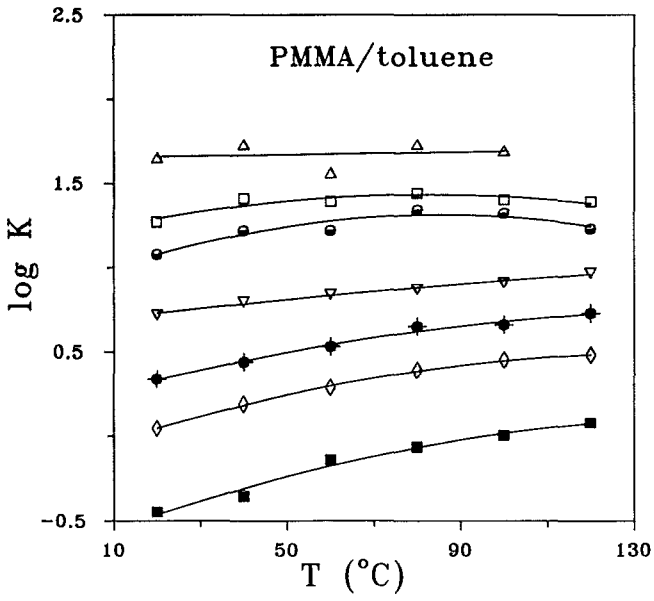

FIG. 7. Temperature dependence of the intensity ratio K, defined as the ratio of the broader (I_2) to the narrower (I_1) spectral component, over a range of PMMA/toluene concentrations (key of Fig. 4).

It is now evident that intensity from the broader component reappears in the narrower component. This suggests that the intensity I_1 contains two contributions: (i) one due to polymer and (ii) one due to slowly relaxing toluene molecules in the vicinity of the PMMA chains. The latter contribution to I_1 increases both with increasing polymer concentration and decreasing temperature. Knowing that there is an intensity interplay ($I_2 \mapsto I_1$) we can now return to Fig. 7 and seek the fraction of I_2 (or, equivalently, the fraction of slowly relaxing toluene) necessary to reproduce the experimental K values. At the highest temperature (120 °C) and for $c_{PMMA} = 0.3$ and 0.7 g/cc we find that 4% and 12%, respectively, of slowly moving toluene molecules can reproduce the experimental K values. At 20 °C, and for $c_{PMMA} = 0.7$ g/cc, this fraction is increased to 21%. Evidently, from the intensity ratio K and, more importantly, from the absolute intensities I_1 and I_2, we are able to obtain the fraction of slower ("modified") solvent molecules in the neighborhood of the polymer chains. This constitutes strong evidence for polymer-induced modification independent of the fitting procedure and furthermore supports the results on the PS/A1248 system[11] at much lower polymer concentrations. The presence of two distinct time scales in the mixed glass is further indicated by the Brillouin and PCS experiments in Sec. III B.

Our results can now be discussed in terms of existing models of rotational relaxation. For high polymer concentrations and low temperatures, the model of restricted rota-

tional diffusion (RRD) (Ref. 37) is usually applied. The RRD model was first suggested by Warchol and Vaughan[38] as a model for the dielectric relaxation of rigid rod molecules trapped in glassy matrices. Wang and Pecora[39] extended the theory to include second-rank spherical harmonic correlation functions and they were able to predict the depolarized light-scattering spectra of molecules undergoing restricted rotational diffusion such as CB (Ref. 6) and *p*-chlorodiphenyl methane (CPM) (Ref. 40) in PMMA. In the framework of this model, two widely separated relaxation time scales exist as a consequence of two types of motion of a rodlike solvent molecule in the polymer matrix. The faster reorientation time (broader interferometric component) arises from restricted rotational diffusion of the solvent in a cavity created by the polymer segments, whereas the slower reorientation time (narrower interferometric component) arises from cooperative motion between the solvent and the polymer segments, thus reflecting a broad distribution of relaxation times which can be analyzed at lower temperatures using PCS. In the RRD model, both the integrated intensity of the narrower and broader components and the dynamics of the broader component depend only on one parameter: the angle of restriction θ_0. Our experimental results shown in Fig. 7 are consistent with the predictions of the RRD model. The ratio K (Fig. 7) decreases both with decreasing temperature and increasing PMMA concentration, i.e., with increasing restriction. The cone angle of rotation of toluene within the PMMA matrix, calculated from the intensity ratio K for the samples with higher c_{PMMA} reveals a temperature dependence (not shown here) similar to K. Analytically, for $c_{\mathrm{PMMA}} = 0.5$ g/cc, θ_0 varies from 52° to 64° in the temperature range 20–120 °C. For $c_{\mathrm{PMMA}} = 0.6$ g/cc the variation is between 41° to 57°, whereas, for $c_{\mathrm{PMMA}} = 0.7$ g/cc, between 25° to 42° in the same temperature range.

Doi[41] described the rotational motion of rodlike polymers in concentrated solutions on the basis of the tube model. The similarities between the Wang–Pecora and the Doi models were previously discussed by Williams.[42] It was also demonstrated that the relaxation times $\tau(l=1)$ and $\tau(l=2)$, can be very similar for restricted rotational diffusion.[42,43] On the other hand, the broad dielectric relaxations observed in the mixtures PS/di-*n*-butyl phthalate and PS/DOP (Ref. 1) could not be explained by either of the two previously mentioned models (Wang–Pecora and Doi). Alternatively, these broad dielectric relaxation processes were qualitatively discussed in terms of the variety of environments for the solvent molecules. In this picture, some molecules are almost free to reorientate their dipole moment in an environment—created by the polymer chains—which does not change its configuration within the time scale of the process.

A recent model of rotational relaxation of small molecules in supercooled liquids predicts a bifurcation into two distinct (α and β), noncompeting relaxation pathways with comparable intensities over a broad range of temperatures. The β relaxation is ascribed to rapid angular diffusion within a long-lived torsional potential well, whereas the random restructuring of the torsional potential itself is associated with the α relaxation. However, as is shown in Fig. 12, the "fast" relaxation process of toluene does not conform to an Arrhenius temperature dependence anticipated for the β-relaxation modes. On the other hand, this can be the result of the restriction imposed by the polymer matrix. In addition, the integrated intensities associated with the two processes are temperature dependent and interelated. Furthermore, the model predicts that the ratio $\tau(l=1)/\tau(l=2)$ is about 1 for the α relaxation. This strong theoretical prediction for the α relaxation has been verified recently[35b] for the solvent DOP and for PS/DOP solutions from DRS and DR measurements made on the same samples.

A statistical-mechanical calculation of the orientation correlation function $\Phi^B_{lm}(t)$ of a solute molecule (B) in a dense liquid of species A has been recently carried out.[13] The second-order function $\Phi^B_{20}(t)$ for an ellipsoidal solute (like toluene) is a superposition of an exponential and, in general, a nonexponential decay function. Whereas, the latter includes the kinetic and thermodynamic contribution of B, the former describes the rotational diffusion of the solute. This molecular theory predicts a bifurcation of the relaxation dynamics of the solute at some temperature $T^* > T_g$ into two processes. The faster mode reflects the characteristics of the solute and the slower (α) process displays dynamic properties of the host medium. Moreover, this model can, in principle, allow for temperature dependence of the intensities of the two processes mainly through the static pair-correlation functions in the system. These theoretical predictions are in accord with the main experimental features of the present study. In fact, the two relaxation branches (see Fig. 12) for the 70% PMMA/toluene sample resemble the PMMA and toluene bare behavior.

B. Polarized Rayleigh–Brillouin scattering

The Rayleigh–Brillouin spectrum of a PMMA/toluene mixture with PMMA concentration of 0.7 g/cc shown in Fig. 2 at 60 °C displays some characteristic features. Although the Brillouin shift (f_B) is intermediate between the corresponding shifts for the pure components, the linewidth ($2\Gamma_B$) is broader than the corresponding linewidth of the pure components, i.e., the mixture exhibits higher hypersonic attenuation. At GHz frequencies, the primary α relaxation contributes to the linewidth at high temperatures [$\sim T_g + 180$ K (Ref. 44)]. However, the spectrum of the mixture in Fig. 2 is only 70 K above T_g (~ -13 °C). This suggests that the observed hypersonic attenuation cannot originate from the α relaxation of the mixed glass. The temperature dependence of the Brillouin shifts for bulk PMMA, neat toluene, and PMMA/toluene mixtures with different PMMA concentrations are shown in Fig. 9. We observe large changes in the compressibility of the system for PMMA concentrations 0.9, 0.8, 0.7, and 0.6 g/cc and smaller changes for $0 < c_{\mathrm{PMMA}} < 0.6$ g/cc. Especially for mixtures with low PMMA concentrations ($0 < c_{\mathrm{PMMA}} < 0.3$), f_B is nearly the same as for neat toluene. Parenthetically, it is noteworthy that this was not the case in a similar study of the blend PMMA/poly(ethylene oxide) (PEO).[7] Apparently, addition of 10% toluene to bulk PMMA affects the compressibility more than addition of the same amount of solvent to a PMMA/toluene mixture with

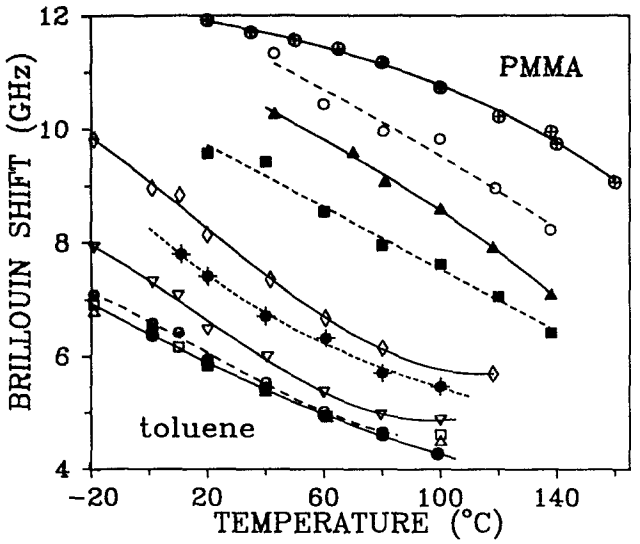

FIG. 9. Brillouin shift vs temperature for PMMA (⊕), toluene (●), and PMMA/toluene solutions with different PMMA concentrations: ○, 0.9; ▲, 0.8, and key of Fig. 4.

low PMMA concentration. Furthermore, the temperature dependence of f_B for $0.7 \leqslant c_{\mathrm{PMMA}} < 1$ resembles the shape of bulk PMMA, whereas $0 < c_{\mathrm{PMMA}} \leqslant 0.6$ resembles the shape of toluene.

Figure 10 shows the temperature dependence of the hypersonic loss $\tan\delta$ ($= 2\Gamma_B/f_B$) for bulk and plasticized PMMA with polymer concentrations 0.9, 0.8, 0.7, and 0.6 g/cc. A pertinent feature of Fig. 10 is the existence of a broad attenuation in all mixed glasses in a temperature range prior to the primary α relaxation which scales with toluene content. It is natural at this point to associate this broad shoulder with relaxation mechanisms related to the solvent.[45] To justify this assumption we will extract a characteristic time

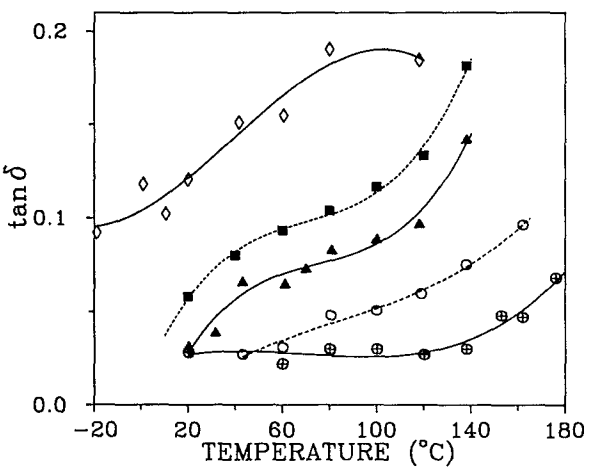

FIG. 10. Hypersonic loss $\tan\delta$ ($= 2\Gamma_B/f_B$) vs temperature for bulk PMMA (⊕) and PMMA/toluene solutions with PMMA concentrations: ○, 0.9; ▲, 0.8; ■, 0.7; ◇, 0.6 g/cc.

from the broad hypersonic attenuation, at GHz frequencies, and compare it with the reorientation times obtained from DRS at zero frequency. In doing so, we estimate the characteristic time τ from the frequency $f_{\max}$ at which $2\Gamma_B$ attains its maximum value τ ($= 1/2\pi f_{\max}$). For the mixture with $c_{\mathrm{PMMA}} = 0.7$ g/cc, we estimate the maximum to occur at 60 °C with a characteristic time $\tau = 1.9\times10^{-11}$ s. At this temperature the neat toluene reorientation time is 4×10^{-12} s, the narrower interferometric component corresponds to 2.2×10^{-9} s and the broader interferometric component to 1.76×10^{-11} s. Evidently, the neat solvent reorientation time is much faster than the characteristic time τ, whereas the narrower component will contribute to the linewidth only at higher temperatures (α relaxation with characteristic time $\tau_{\alpha,\max}$). On the other hand, the dynamics of the broader interferometric component agree within 5% with the time τ.

For the PMMA/toluene mixture with $c_{\mathrm{PMMA}} = 0.6$ g/cc, a broad hypersonic attenuation is observed which exhibits a maximum value at a temperature $T_{\max} \sim T_g + 180$ K or equivalently when $f_B \sim 5$–6 GHz, then the $\tan\delta$ maximum for the primary relaxation should occur at ~ 137 K. Again, the residual low-temperature attenuation ($\tan\delta = 0.1$ at -20 °C) is not due to the α relaxation. The broad hypersonic attenuation exhibited by the mixed glass can arise from the presence of two relaxations. As with the former PMMA/toluene mixture ($c_{\mathrm{PMMA}} = 0.7$ g/cc), we estimate the maximum at ~ 20 °C resulting in a characteristic time of 1.96×10^{-11} s. This time compares well with the solvent reorientation time of the broader interferometric component (1.71×10^{-11} s at 20 °C). At the same temperature the neat solvent reorientation time is 5.6×10^{-12} s. Figure 10 provides adequate evidence that the low-temperature shoulder in the PMMA/toluene mixtures with PMMA concentration: 0.9, 0.8, 0.7, and 0.6 g/cc is associated with the mobile solvent which possesses sufficient rotational mobility in the mixed glass.

An important quantity in the discussion of the Rayleigh–Brillouin spectra is the Landau–Placzek (LP) intensity ratio, shown in Fig. 11 for neat toluene and four PMMA/toluene mixtures. Its value is usually overestimated as any parasitic elastically scattered light contributes to the intensity of the central Rayleigh line. A reliable measurement of LP requires samples of high optical quality. For polymer solutions, the value of LP is usually overwhelmed by the concentration fluctuations which dominate the light-scattering intensity. Only for perfect optical matching is this contribution really suppressed. The LP ratio due to density fluctuations is given by[46]

$$\mathrm{LP} = \gamma \frac{M'(\omega)}{M_0} - 1, \tag{8}$$

where $M'(\omega)$ is the real part of the adiabatic longitudinal modulus at frequency ω, M_0 is the longitudinal modulus at zero frequency (high temperature), and γ is the ratio of the specific heats at constant pressure and volume. According to Eq. (8), the LP should increase monotonically with decreasing temperature from the thermodynamic limit $\gamma - 1$ to $\gamma(M_\infty/M_0) - 1$, with M_∞ being the high-frequency limit-

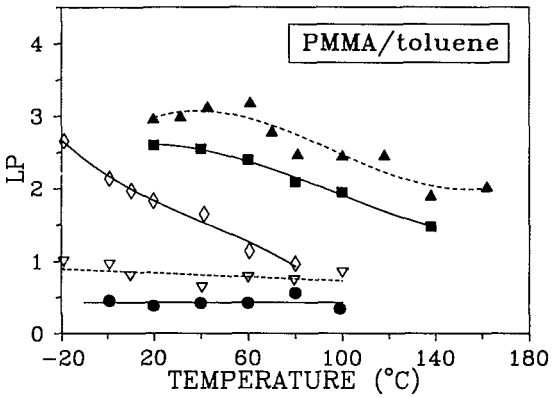

FIG. 11. Temperature dependence of the Landau–Placzek (LP) intensity ratio of toluene (●) and PMMA/toluene solutions with PMMA concentrations: ▽, 0.4; ◇, 0.6; ■, 0.7; ▲, 0.8 g/cc.

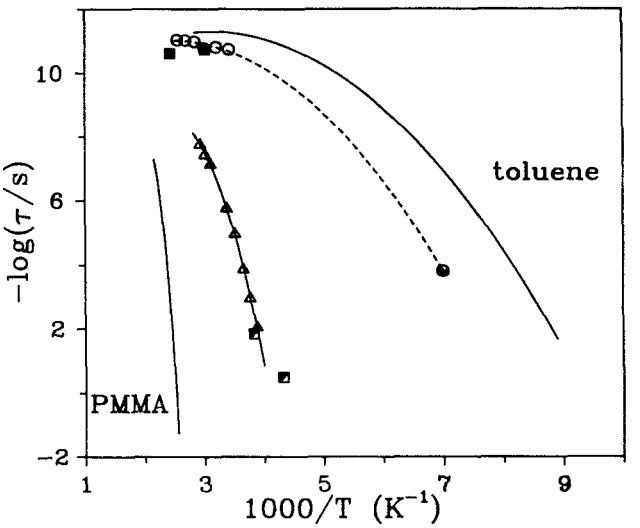

FIG. 12. Temperature dependence of the "fast" (broken line) and "slow" (solid line) relaxation processes in a PMMA/toluene mixture with $c_{PMMA} = 0.7$ g/cc. The fast process is determined from DRS (○), FPI (○), and DR (◒) and the slow process from PCS (◩) and DR (△). The estimated FPI maximum due to the α relaxation is also shown (■). The "fast" and "slow" relaxation processes can be compared, respectively, with the neat toluene and bulk PMMA relaxations, also shown.

ing value of the modulus. Usually the temperature dependence of LP reveals a sigmoidal shape as a result of a dispersion mechanism which makes some degrees of freedom become inactive at hypersonic frequencies. For toluene, this ratio is constant and is about 0.5 and exceeds $(\gamma - 1)$ the fast relaxation limit $(\omega\tau \ll 1)$ due to the effect of internal relaxations. For the PMMA/toluene mixture with $c_{PMMA} = 0.4$ g/cc, the LP is still low but higher than for neat toluene, either because of the contribution of concentration fluctuations (not ideal optical matching) or the existence of fast structural relaxation. The latter is more likely in view of the consistent further increase of LP with c_{PMMA} and its temperature dependence as shown in Fig. 11. Moreover, this variation of LP with temperature is in accord with the hypersonic absorption data of Fig. 10, which strongly hind at significant dispersion, i.e., $M'/M_0 > 1$. Based mainly on the account for the temperature dependence of tan δ, the behavior of the LP ratio corroborates the notion of two structural relaxations assigned to "mobile" toluene and plasticized PMMA dynamics. The latter slow (α) relaxation is probably responsible for the finding that the LP of the mixtures with $c_{PMMA} = 0.7$ and 0.8 g/cc remains large at high temperature.

3. Comparison to other relaxation data

Despite the strong evidence of two types of solvent reorientational motion, based mainly on the data of Fig. 8 and Figs. 10 and 11, the slow relaxation process (with characteristic time τ_1 from depolarized and $\tau_{\alpha,\max}$ from polarized scattering) is still poorly characterized from FPI. This is because of the frequency range or the very high temperature required (Fig. 10). We have therefore employed PCS (Ref. 47) in the time range 10^{-6}–10^{3} s to analyze the orientational dynamics of the PMMA/toluene system. The broad time-correlation function $C_{VH}(t)$ is clearly dominated by two relaxation processes from which the slower can be now well analyzed.

Figure 12 shows the characteristic time scale for the two different relaxation processes in PMMA/toluene with $c_{PMMA} = 0.7$ g/cc as obtained from the different light-scattering (FPI, PCS) and dielectric relaxation[22] techniques. The temperature dependence of the primary (α) relaxation times of pure toluene [Eq. (6)] and bulk PMMA (Ref. 48) is also displayed in Fig. 12 for comparison. The DR measurements on similar PMMA/toluene mixtures revealed the presence of three relaxations $(\alpha, \beta,$ and $\gamma)$.[22] These processes were assigned, respectively, to slow segmental dynamics of PMMA which possesses high dipole moment, rotation of toluene molecules, and secondary local motion of toluene molecules. On the contrary, in the depolarized light-scattering experiment, PMMA is almost invisible and the observation of this slow process is possible through the "modified" PMMA anisotropic toluene. In other words, the orientation of the "modified" solvent is determined by the segmental dynamics of the polymeric solute.

The transition map of Fig. 12 is a nice demonstration of the vastly different time scales in the homogeneous PMMA/toluene mixture ($c_{PMMA} = 0.7$ g/cc) exhibiting a single glass transition. The non-Arrhenius temperature dependencies of the "slow" and "fast" processes are closer to the α relaxation of bulk PMMA and neat toluene, respectively, supporting the proposition in the preceding sections. In fact, the "slow" and "fast" relaxation processes in Fig. 12 conform to Eq. (6) with $B = 773 \pm 20$ K, $T_0 = 188 \pm 2$ K and $B = 273 \pm 30$ K, $T_0 = 110 \pm 5$ K, respectively. This finding is in accord with the predictions of the recent molecular theory of Bagchi, Chandra, and Rice.[13] Bifurcation of the solute B (toluene) orientational dynamics occurs at $T^* > T_g$, when the ratio of the rotational diffusion rates D_R^B/D_R^A of the solute and the host (A) medium (PMMA) is

larger than about 50 (Fig. 3 of Ref. 13). In this context, it will be useful to investigate the rotational dynamics of toluene in different polymeric matrices. Existing fluorescence anisotropy[49] and NMR[50] data which are mainly concerned with the polymer segmental dynamics in toluene and DRS data on the toluene reorientation in polystyrene[5] provide the background for this investigation.

IV. CONCLUDING REMARKS

Depolarized Rayleigh and polarized Rayleigh–Brillouin experiments have been used to investigate solvent relaxation in toluene solutions of PMMA. The low Landau–Placzek ratio of all samples used in the present study and the high difference in the optical anisotropies between the polymer and the solvent make the PMMA/toluene system ideal for the investigation of solvent relaxation in a polymer matrix.

The depolarized Rayleigh spectra obtained in the temperature range 20–120 °C were described by a single Lorentzian plus a baseline for toluene, whereas two Lorentzians were necessary to fit the depolarized spectra of the solutions. From the two spectral components in the PMMA/toluene solutions, the broader one reflects the fast solvent reorientation and the narrower one contains contributions from both slowly relaxing polymer chains and slow solvent reorientation in the vicinity of the polymer chains. The integrated intensities of the two spectral components, their ratio K, and the corresponding dynamics are discussed in terms of existing models of rotational diffusion and a recent molecular theory of orientational relaxation of a solute in a supercooled liquid. The most remarkable features of the orientational dynamics of toluene in PMMA concern the normalized solvent relaxation τ/τ_0 and the presence of two distinct relaxation processes below some temperature. The value of τ/τ_0 exhibits an exponential dependence on concentration for PMMA concentration up to 0.7 g/cc at the high interferometric temperatures. To our knowledge, this is the highest concentration for which this prediction is verified. Furthermore, τ/τ_0 is independent of the hydrodynamic volume of the solvent at the high interferometric temperatures and for the three solvents employed in the present system. Moreover, the "fast" and "slow" relaxation processes in the PMMA/toluene mixture with $c_{\mathrm{PMMA}} = 0.7$ g/cc resemble the solute and polymer matrix bare dynamics, respectively, in agreement with recent theoretical predictions.

The polarized Rayleigh–Brillouin measurements revealed the presence of significant dispersion, increasing with toluene content, in a temperature range not affected by the primary relaxation. The molecular mechanism behind this hypersonic attenuation is activated through the mobile solvent which possesses significant rotational mobility as inferred from DRS.

ACKNOWLEDGMENTS

Support by the Research Center of Crete and the Swedish Natural Science Research Council (W.B.) is gratefully acknowledged. Dr. Ladislav Dvoranek of the Institute of Macromolecular Chemistry, Czechoslovak Academy of Sciences, Czechoslovakia, kindly supplied the PMMA/toluene samples. G. Floudas acknowledges the Institute of Physical Chemistry, University of Uppsala, for its hospitality.

[1] P. J. Hains and G. Williams, Polymer **16**, 725 (1975).
[2] K. Adachi, I. Fujihara, and Y. Ishida, J. Polym. Sci. Polym. Phys. Ed. **13**, 2155 (1975).
[3] E. Rössler, H. Sillescu, and H. W. Spiess, Polymer **26**, 203 (1985).
[4] C. Zhang, P. Wang, A. A. Jones, P. T. Inglefield, and R. P. Kambour, Macromolecules **24**, 338 (1991).
[5] G. D. Patterson, C. P. Lindsey, and G. R. Alms, Macromolecules **11**, 1242 (1978).
[6] A. C. Ouano and R. Pecora, Macromolecules **13**, 1167 (1980).
[7] G. Fytas, J. Kanetakis, G. Floudas, and C. H. Wang, Polym. Commun. **31**, 434 (1990).
[8] T. P. Lodge and J. L. Schrag, Macromolecules **17**, 352 (1984).
[9] M. G. Minnick and J. L. Schrag, Macromolecules **13**, 1690 (1980).
[10] R. L. Morris, S. Amelar, and T. P. Lodge, J. Chem. Phys. **89**, 6523 (1988).
[11] G. Fytas, A. Rizos, G. Floudas, and T. P. Lodge, J. Chem. Phys. **93**, 5096 (1990).
[12] M. Fixman, J. Chem. Phys. **92**, 6858 (1990).
[13] B. Bagchi, A. Chandra, and S. A. Rice, J. Chem. Phys. **93**, 8991 (1990).
[14] S.-B. Zhu and G. W. Robinson, J. Chem. Phys. **90**, 7127 (1989).
[15] A. Rizos, G. Fytas, T. P. Lodge, and K. L. Ngai, J. Chem. Phys. (to be published).
[16] B. Berne and R. Pecora, *Dynamic Light Scattering* (Wiley-Interscience, New York, 1976).
[17] G. Floudas, A. Patkowski, G. Fytas, and M. Ballauff, J. Phys. Chem. **94**, 3215 (1990).
[18] Y. Koike, N. Tanio, and Y. Ohtsuka, Macromolecules **22**, 1367 (1989).
[19] G. D. Patterson, P. K. Jue, and J. R. Stevens, J. Polym. Sci. Polym. Phys. Ed. 28, **481** (1990).
[20] W. Brown, K. Schillen, R. Johnsen, C. Konak, and L. Dvoranek, Macromolecules (in press).
[21] See, for example, J. L. Gomez Ribelles, R. Diaz-Calleja, R. Ferguson, and J. M. G. Cowie, Polymer **28**, 2262 (1987).
[22] K. Adachi and T. Kotaka, Polym. J. **13**, 687 (1981).
[23] H. C. Andersen and R. Pecora, J. Chem. Phys. **54**, 2584 (1971); G. D. Patterson and G. R. Alms, Macromolecules **10**, 1237 (1977).
[24] C. Levy and G. D'Arrigo, Mol. Phys. **50**, 917 (1983).
[25] T. Keyes and D. Kivelson, J. Chem. Phys. **56**, 1057 (1974).
[26] E. Rössler, J. Chem. Phys. **92**, 3725 (1990).
[27] E. Rössler, Phys. Rev. Lett. **65**, 1595 (1990).
[28] E. Leutheusser, Phys. Rev. A **29**, 2765 (1984); U. Bengtzelius, W. Götze, and A. Sjölander, J. Phys. C **17**, 5915 (1984); W. Götze, Phys. Scr. **34**, 66 (1986).
[29] C.-M. Hu and R. Zwanzig, J. Chem. Phys. **60**, 4354 (1974).
[30] A. J. Barlow, J. Lamb, and A. J. Matheson, Proc. R. Soc. London, Ser. A **292**, 322 (1966).
[31] G. R. Alms, D. R. Bauer, J. I. Brauman, and R. Pecora, J. Chem. Phys. **58**, 5570 (1973).
[32] E. Rössler and H. Sillescu, Chem. Phys. Lett. **112**, 94 (1984).
[33] D. Kivelson and S. A. Kivelson, J. Chem. Phys. **90**, 4464 (1989).
[34] G. R. Alms, G. D. Patterson, and J. R. Stevens, J. Chem. Phys. **70**, 2145 (1979).
[35] (a) G. Floudas, Ph.D. thesis, University of Crete, 1990; (b) G. Fytas, G. Floudas, W. Steffen, and L. Giebel (unpublished).
[36] A. Rizos (private communication).
[37] A. C. Ouano and R. Pecora, Macromolecules **13**, 1173 (1980).
[38] M. P. Warchol and W. E. Vaughan, Ad. Mol. Relaxation Interact. Proc. **13**, 317 (1978).
[39] C. H. Wang and R. Pecora, J. Chem. Phys. **72**, 5333 (1980).
[40] N. H. Oliver, R. Pecora, and A. C. Ouano, Macromolecules **18**, 2208 (1985).
[41] M. Doi, J. Polym. Sci. Polym. Phys. Ed. **20**, 1963 (1982).
[42] G. Williams, J. Polym. Sci. Polym. Phys. Ed. **21**, 2037 (1983).
[43] G. Williams (private communication).
[44] J. P. Jarry and G. D. Patterson, J. Polym. Sci. Polym. Phys. Ed. **19**, 179 (1981).
[45] Another mechanism of hypersonic attenuation, i.e., the translational-vibrational (T-V) coupling present in toluene has only very weak ($T^{1/3}$)

temperature dependence and, hence, cannot account for the shoulder in Fig. 10 [Th. Dorfmüller, G. Fytas, W. Mersch, and D. Samios, J. Chem. Soc. Faraday Discuss. II **11**, 106 (1977)].
[46] D. A. Pinnow, S. J. Candau, J. T. LaMacchia, and T. A. Litovitz, J. Acoust. Soc. Am. **43**, 131 (1967).
[47] G. Floudas and G. Fytas, Coll. Polym. Sci. (to be published).
[48] G. Fytas, C. H. Wang, and E. W. Fischer, Macromolecules **21**, 2253 (1988).
[49] D. A. Waldow, B. S. Johnson, P. D. Hyde, M. D. Ediger, T. Kitano, and K. Ito, Macromolecules **22**, 1345 (1989).
[50] D. J. Gisser, S. Glowinkowski, and M. D. Ediger, Macromolecules **24**, 4270 (1991).